Optimizing PEG Molecular Weight and Molar Composition for Enhanced *In Vivo* Pharmacokinetics of a Mixed Micellar siRNA Carrier

By

Martina Miteva

Thesis

Submitted to the Faculty of the

Graduate School of Vanderbilt University

in partial fulfillment of the requirements

for the degree of

MASTER OF SCIENCE

in

Biomedical Engineering

December, 2013

Nashville, TN

Approved:

Craig L. Duvall, Ph.D.

Todd D. Giorgio, Ph.D.

ACKNOWLEDGEMENTS

This work was made possible with the financial support of DOD CDMRP Collaborative Idea Expansion Awards: W81XWH-10-1-0446/-0445 and the IBM Graduate Fellowship. Experiments were in part performed using equipment in the Vanderbilt University Institute of Imaging Sciences (VUIIS) and in the Vanderbilt Institute of Nanoscale Science and Engineering (VINSE). I would like to thank my advisors, Dr. Todd D. Giorgio and Dr. Craig L. Duvall, for their ongoing support, enthusiasm, and expertise in the field. Additionally, I would like to thank Dr. Hongmei Li, Dr. Kellye Kirkbride and Chris Nelson for their assistance and guidance throughout this project.

TABLE OF CONTENTS

LIST OF TABLES

Tables **Page**

LIST OF FIGURES

Figures **Page**

CHAPTER I

INTRODUCTION

RNA interference (RNAi) by small interfering RNA (siRNA) has potential to be applied therapeutically to treat cancer or other pathologies whose etiology is related to aberrant gene overexpression [1]–[3]. siRNA is a class of 20-25 base pair double-stranded RNA that is able to cause post-transcriptional gene silencing following introduction and intracellular uptake [1]. Following cellular uptake into the cytoplasm, the double-stranded siRNA is cleaved, and a single strand, known as the guide strand, loads onto the RNA-induced silencing complex (RISC), while the passenger strand is cleaved by Argonaute-2. The RISC then uses the guide strand to identify and hybridize to the mRNA to be cleaved (Figure 1) [4]. In literature, siRNA has previously been injected directly to the eye for local gene silencing of human endothelial growth factor (VEGF) [5]. However, systemic administration of siRNA is limited by the small size of siRNA, which often leads to premature degradation by nucleases and renal clearance, while its negative charge provides a barrier to significant delivery through the cationic cellular surface. Due to these poor pharmacokinetic properties, siRNA requires a

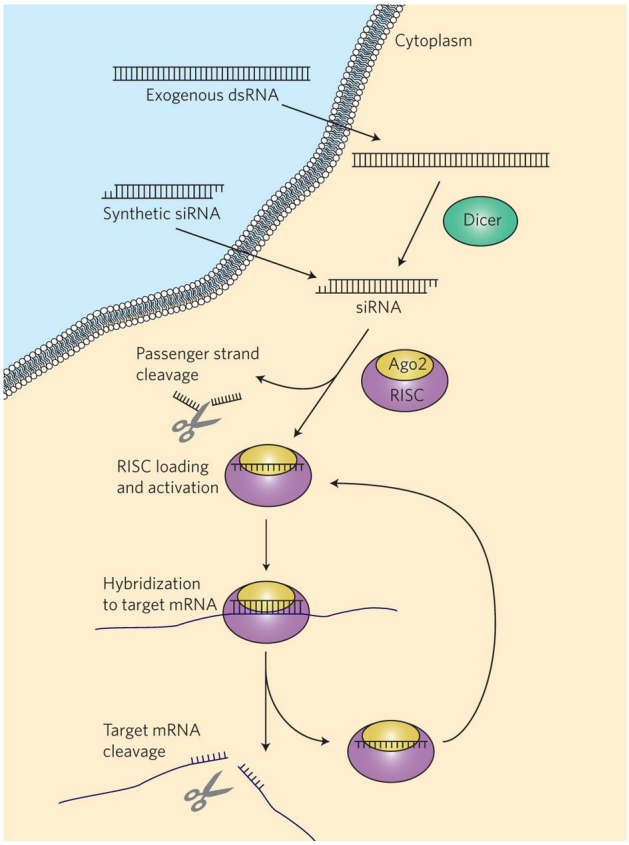

Figure 1. Mechanism of RISC-induced cleavage of mRNA following transcription (adapted from Kanasty et al. [4]**)**

carrier for effective intracellular delivery [6].

Cationic polymers that electrostatically condense siRNA have been widely studied as carriers that are able to protect siRNA from degradation while effectively penetrating the cell surface for intracellular delivery [7]–[9]. Many of these net positively charged carriers have demonstrated activity *in vitro*, but they often have poor hemocompatibility when injected intravenously *in vivo,* which can lead to unexpected toxicity [10]. Particles electrostatically assembled from cationic polymers and siRNA become unstable, nonspecifically bind with blood plasma proteins, which causes formation of erythrocyte aggregates that can accumulate within and block the pulmonary vasculature [11], [12]. Polyplexes of siRNA with cationic polymers can also be destabilized through interactions with anionic heparan sulfate in the glomerular basement membrane (GBM), leading to rapid renal excretion and hindered ability to generate RNAi within the intended tissue[13], [14].

Here, a pH-responsive diblock copolymer-based micelle previously established for *in vitro* delivery of siRNA [15], [16] was utilized as the base delivery system. This micelleplex system is self-assembled from a diblock polymer consisting of a pH-responsive, endosomolytic core-forming block composed of butyl methacrylate (BMA), propyl acrylic acid (PAA), and dimethylaminoethyl methacrylate (DMAEMA) and a corona-forming poly(DMAEMA) (pDMAEMA) block, which is positively charged at pH 7.4 and condenses anionic siRNA (Figure 2). The micelle has a high positive surface charge, however, that hinders its ability to be

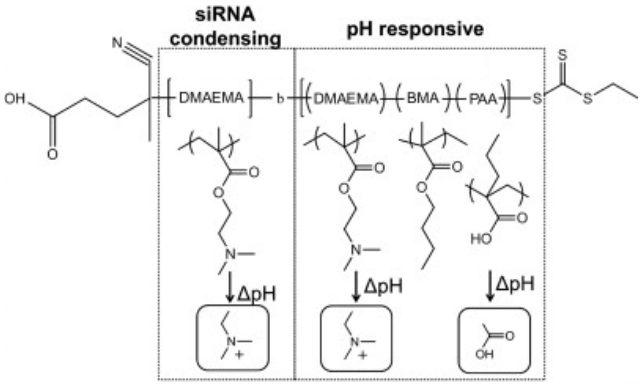

Figure 2. Cationic diblock micelle-forming siRNA delivery polymer. Figure adapted with permission from [23]**.**

directly translated for intravenous use *in vivo*. In order to overcome this limitation, a series of micelles have been designed that leverage the same endosomolytic terpolymer core but that possess mixed coronas composed of DMAEMA and varied quantities and molecular weight poly(ethylene glycol) (PEG). PEG was utilized because of its known beneficial effects on biocompatibility, stability, pharmacokinetics, and biodistribution of drug nanocarriers [17]–[21].

Here, these new micelles were characterized *in vitro* for stability, hemocompatibilty, cellular uptake, and siRNA delivery efficacy and *in vivo* in mouse models to determine tissue biodistribution and blood circulation half-life. By optimizing the molecular weight and surface concentration of PEG on the corona of these mixed micelles, we have created a stable and effective siRNA carrier with a significantly improved blood circulation half-life that can be leveraged for enhanced permeability and retention (EPR) effect-based tumor delivery [22].

CHAPTER II

MATERIALS AND METHODS

Materials

All chemicals were purchased from Sigma-Aldrich Co. (St Louis, MO, USA) unless otherwise noted. The 10 kDa methoxy-poly(ethylene glycol) (mPEG) was purchased from CreativePEGWorks (Salem, NC, USA), and the 20 kDa mPEG was purchased from JemKem USA (Plano, TX, USA). Hiperfect transfection reagent was purchased from Qiagen (Hilden, Germany).

Cell Culture

MDA-MB-231 and NIH-3T3 cells were purchased from ATCC (Manassas, VA, USA). MDA-MB-231 and RFP-231 (MDA-MB-231 cells that had been stably transfected with a firefly luciferase reporter gene) were cultured in DMEM (Gibco, Carlsbad, CA) with 10% FBS (Gibco, Carlsbad, CA) and 50 ug/mL gentamicin (Gibco, Carlsbad, CA). NIH 3T3s were cultured in DMEM + 10% FBS and 1% P/S.

Polymer synthesis and characterization

All polymers were synthesized by reversible addition fragmentation chain transfer (RAFT) polymerization.

Synthesis of 5k and 10k PEG macro chain transfer agent (macroCTA)

The PEG macroCTAs were synthesized by adding dicyclohexylcarbodimide (DCC, 1 mmol) to a stirring solution of mono mPEG (250 umol), ethyl cyanovaleric trithiocarbonate (ECT, 500

umol) and 4-Dimethylaminopyridine (DMAP, 50 umol) in anhydrous dichloromethane. The reaction mixture was stirred for 48 hours under a nitrogen atmosphere. The precipitated cyclohexyl urea was removed by filtration, and the dichloromethane layer was concentrated and precipitated into diethyl ether twice. The precipitated polymer was washed three times with diethyl ether and dried under vacuum overnight. ^{1}H nuclear magnetic resonance (NMR) spectra showed that 90% of the 10k PEG was conjugated with ECT, and 84% of the 5k PEG was conjugated with ECT.

Synthesis of diblock PEG-b-(DMAEMA-co-PAA-co-BMA)

The diblock polymer 5k PEG-b-(DMAEMA-co-PAA-co-BMA) (PEG-b-DPB) was synthesized via RAFT polymerization. The monomers were added to the 5k PEG macroCTA at stoichiometric quantities of 50% BMA, 25% DMAEMA, and 25% PAA at a monomer to CTA molar ratio of 400. The initiator azobisisobutyronitrile (AIBN) was added at a CTA to initiator molar ratio of 20 in a mixture of dioxane and DMF as the solvent. The polymerization was stirred for 24 hours at 70°C under a nitrogen atmosphere. The resulting polymer was precipitated in 50% ether and 50% pentane three times, followed by drying under vacuum overnight. The same conditions were used to synthesize and precipitate the 10k PEG-b-DPB.

The 20k PEG-b-DPB was synthesized by RAFT by adding monomers in a stoichiometric ratio of 50% BMA, 25% DMAEMA, and 25% PAA to the 20k PEG macroCTA at a monomer to CTA ratio of 800. Initiator AIBN was added at a CTA to initiator ratio of 8.33. Polymerization was stirred over 24 hours in dioxane and DMF under a nitrogen atmosphere. The resulting polymer was precipitated in the same way as the 5k PEG-b-DPB and 10k PEG-b-DPB.

Synthesis of pDMAEMA macroCTA

The pDMAEMA macroCTA was synthesized via RAFT polymerization as previously described [15], [23]. Briefly, DMAEMA monomer was added to the ECT at a monomer to CTA ratio of 100, and the initiator AIBN was added at a CTA to initiator ratio of 10. The reaction was stirred over 6 hours at 70°C in DMF under a nitrogen atmosphere. The resulting polymer was precipitated in pentane three times and dried under vacuum overnight.

Synthesis of diblock DMAEMA-b-(DMAEMA-co-PAA-co-BMA)

The diblock polymer DMAEMA-b-(DMAEMA-co-PAA-co-BMA) (D-b-DPB) was synthesized via a RAFT polymerization as previously described [15], [23]. Briefly, monomers were added to pDMAEMA macroCTA at stoichiometric quantities of 50% BMA, 25% DMAEMA and 25% PAA at a monomer to CTA ratio of 250. The initiator AIBN was added at a CTA to initiator ratio of 5. Polymerization was stirred at 70°C for 24 hours under a nitrogen atmosphere. The resulting polymer was precipitated in 50% ether and 50% pentane three times and dried overnight under vacuum. It was then dissolved in a minimal volume of 100% ethanol, further diluted into dH_2O, and purified through a PD10 desalting column (GE Healthcare). The eluent was lyophilized.

Polymer characterization

To determine molecular composition of the polymers, ^1H NMR was performed in $CDCl_3$ using a Bruker 400 MHz spectrometer. To determine molecular weight and polydispersity, gel permeation chromatography (GPC) was performed on the polymers in filtered dimethyl formamide (DMF) containing 0.1 M lithium bromide (LiBr) on an Agilent Infinity GPC. The

dn/dc values used to calculate absolute molecular weight were determined on the same instrument by direct injections of polymer solutions into the RI detector.

Micelle formation and characterization

Micelles were formed by solvent exchange. Lyophilized diblock polymers of the desired characteristics and stoichiometry were weighed out and dissolved together in a minimal volume of pure ethanol. PBS was then slowly added to the dissolved polymers using a syringe pump at a rate of 8 mL/hour. The final micelle solution was 2 mg/ml and contained 1% ethanol. Micelles were filtered through a 0.45 um syringe filter and dynamic light scattering (DLS) measurements were performed on a Malvern Zetasizer Nano-ZS (Malvern Instruments Ltd, Worcestershire, U.K). Zeta (ζ) potential was also determined on the same instrument. Transmission electron microscopy (TEM) images were acquired using a Philips CM20 HR-TEM (Philips, EO, Netherlands). TEM samples were prepared by quickly adding a drop of 1 mg/ml micelle solution on a copper grid and staining the grid briefly with uranyl acetate. The grid was then allowed to dry under vacuum overnight before imaging.

siRNA loading determination by gel electrophoresis

siRNA loading of micelles was determined by gel electrophoresis. Briefly, micelles were complexed with siRNA over a range of N+/P- charge ratios for roughly 1 hour. N+/P- ratios were determined by using the positive charge due to the pDMAEMA, which is assumed to be 50% protonated at pH 7.4, divided by the negative charge due to 21 base pair, double-stranded siRNA. After siRNA complexation, micelles were mixed with loading dye and were run alongside a 20 base pair molecular ladder on a 2% agarose gel.

Red blood cell hemolysis assay

A red blood cell hemolysis assay to determine endosomolytic behavior of the micelles was performed as previously described [24]. Briefly, varying concentrations of micelles were incubated with fresh anticoagulated human red blood cells suspended in a range of pHs that represent extracellular, early endosome, late endosome, and lysosome pH (7.4, 6.8, 6.2, and 5.6, respectively), in a 96 well plate for an hour at 37°C. After incubation, the plate was centrifuged at 500xg for 5 minutes. 100 uL of supernatant was transferred to a clear bottom 96 well plate and absorbance at 595 nm was determined on a plate reader (Tecan Group Ltd, Mannedorf, Switzerland).

Whole blood interaction assay

The hemocompatibility of the micelles was determined by performing a whole blood aggregation assay as previously described [25]. Micelles were complexed with Cy5-labeled double stranded DNA (dsDNA) (Sigma-Aldrich Co., St. Louis, MO, USA), used as a model molecule for double stranded siRNA, at an N+/P- ratio of 6. The complexes were then added to dilute human whole blood for a final siRNA concentration of 200 nM in a 96-well plate. As a control, the micelles were also added to PBS for a final siRNA concentration of 200 nM. The formulations were placed on a shaker for 5 minutes before incubation at 37°C for an hour. The plates were then centrifuged at 500xg for 5 minutes. 100 uL of supernatant from each well was transferred to a black, clear bottom 96-well plate and Cy5 fluorescence was measured on a plate reader (Tecan Group Ltd, Mannedorf, Switzerland).

Measurement of stability in presence of heparin

Heparin sodium salt acts as a model for competing polyanions that are present *in vivo* and within cells. Micelles were complexed with double stranded siRNA at an N+/P- ratio of 6 for an hour. The complexes were then added to a black, clear-bottom 96 well plate at a final concentration of 100 nM with 250 U/L heparin sodium salt in PBS in a total volume of 100 uL. Dilute Quant-iT RiboGreen RNA Reagent (Life Technologies, Grand Island, NY, USA) was added per manufacturer's instructions to the mixture for a total final volume of 200 uL. RiboGreen fluorescence (excitation of 488 nm, emission of 520 nm) was measured over two hours on a plate reader (Tecan Group Ltd, Mannedorf, Switzerland), and percent siRNA released from the micelles was determined by calculating percent fluorescence normalized to fluorescence of an equivalent concentration of free siRNA.

Assessment of siRNA protection from degradation

The hyperchromic effect describes an observed increase in absorbance at 260 nm when nucleic material degrades. This phenomenon was used to determine the micelles' ability to protect siRNA against nuclease degradation as previously described [26], [27]. Micelles were complexed to double-stranded siRNA at a N+/P- ratio of 6. The micelles were then diluted in 100 uL of dH_2O for a final siRNA concentration of 500 nM and placed in a small volume quartz cuvette. Then, 300 nU of Riboshredder RNAse Blend (Epicentre, Madison, WI, USA) was added and absorbance at 260 nm was kinetically monitored for 20 minutes on a Cary 100 UV-vis spectrophotometer (Agilent Technologies, Santa Clara, CA, USA).

Cellular uptake by flow cytometry

Cellular uptake of the micelles by MDA-MB-231 mammary epithelial cells was determined by flow cytometry as previously described [28]. Briefly, MDA-MB-231 cells were seeded on 24-well plate in media supplemented with 1% FBS and were allowed to adhere overnight. Micelles were complexed with AlexaFluor488-labeled dsDNA at an N+/P- ratio of 6 for an hour. Cells were then treated with micelleplexes at a dsDNA concentration of 100 nM for 6, 12, and 24 hours. Immediately after treatment, cells were washed with PBS and trypsinized. Following trypsinization, cells were centrifuged and cell pellets were re-suspended in 0.05% trypan blue solution to quench extracellular fluorescence. Cell fluorescence was measured via flow cytometry (FACSCalibur, BD Biosciences, Franklin Lakes, NJ) and analyzed using FlowJo software.

Cytotoxicity assessment

Cellular viability was measured in luciferase-expressing NIH-3T3 cells (Luc-3T3s) after treatment with micelles. Luc-3T3 cells were seeded on a black, clear bottom 96-well plate and allowed to adhere overnight. Micelles were complexed with scrambled siRNA at a N+/P- ratio of 6. Cells were treated for 6, 12, and 24 hours at a concentration of 100 nM siRNA. Immediately following treatments, media was removed and cells were washed once with PBS. Fresh media containing luciferin was added to the cells, and the bioluminescence was measured on the IVIS Imaging System (Xenogen Corporation, Alameda, CA, USA).

siRNA gene knockdown

RFP-231 cells (MDA-MB-231 cells that were virally transfected to constitutively express luciferase) were seeded in a black, clear-bottom 96-well plate in media supplemented with 1% FBS and allowed to adhere overnight. Micelles were complexed with anti-luciferase siRNA (Ambion model #AM4629) at an N+/P- ratio of 6, and cells were treated with micelleplexes for 6, 12, and 24 hours. At the end of the designated treatment times, cells were washed with PBS, fresh media containing 1% FBS was added, and the cells were incubated for an additional 48 hours. Following incubation, media was replaced with luciferin-containing media and bioluminescence was measured using an IVIS Imaging System (Xenogen Corporation, Alameda, CA, USA). Bioluminescence data was normalized to total cellular protein as determined using a Bradford Assay (Bio-Rad Laboratories Inc., Hercules, CA, USA).

***In vivo* half-life determination**

Micelles were complexed to IRDye800-labeled dsDNA for an hour at a N+/P- ratio of 6. Five BALB/c mice (6-8 weeks old) (Charles Rivers Laboratories, Wilmington, MA, USA) were injected in the tail vein with 2 mg/kg (normalized to dsDNA dose) micelleplexes. Blood was retro-orbitally collected at 5 and 10 minutes post-injection (not to exceed two collections per animal). At 20 minutes post-injection, animals were sacrificed, and blood was immediately collected from the renal vein. Collected blood was centrifuged at 500xg for 5 minutes, and 5 uL of plasma supernatant was collected and diluted into 95 uL dH_2O. Fluorescence was measured on a plate reader (Tecan Group Ltd., Mannedorf, Switzerland) at an excitation wavelength of 810 +/- 2.5 nm and an emission wavelength of 790 +/- 5 nm. A standard curve was produced by measuring the fluorescence of the complexes in dH_2O over the range of 200% to 6.25% of initial

injected dose. This standard was utilized to calculate the percent of injected dose in each blood sample, and these calculated values were used to determine blood circulation half-life.

In vivo biodistribution

Animals were injected with dsDNA micelleplexes as stated for the determination of blood circulation half-life. 20 minutes post-injection, animals were sacrificed and organs of interest were excised. Lungs, heart, spleen, liver, and kidneys were excised and fluorescently imaged on the IVIS Imaging System (Xenogen Corporation, Alameda, CA, USA). The different organs were separated into regions of interest (ROI), and the total fluorescence in each region was quantified.

Statistical Analysis

All data are reported as mean +/- standard error of the mean (SEM). ANOVA was used for statistical analysis, and Tukey's post-hoc test was used to determine pairwise significance based on an alpha value of 0.05.

Ethics Statement

All animals in the study were treated humanely under conditions outlined by National Health Institute (NIH). Experiments performed on the animals were approved by Vanderbilt University's Institutional Animal Care and Use Committee (IACUC). Human blood was collected from anonymous donors following a protocol approved by the Vanderbilt Institutional Review Board (IRB).

CHAPTER III

RESULTS AND DISCUSSION

Polymer synthesis and characterization

Four different diblock polymers were synthesized by RAFT polymerization. All four polymers contained a hydrophobic, pH-responsive block consisting of approximately 50% BMA, 25% PAA, and 25% DMAEMA, with a second PEG or DMAEMA block (Table 1). The hydrophobic block was approximately 20 kDa for all polymers except for the polymer containing the 20 kDa PEG, which has a longer hydrophobic block to ensure stable micelle formation despite the large hydrophillic block.

The relative molar percentages of 5k PEG-b-DPB and D-b-DPB polymers were modulated to produce four mixed micelles: 100% D-b-DPB, 75% D-b-DPB / 25% PEG-b-DPB, 50% D-b-DPB / 50% PEG-b-DPB and 25% D-b-DPB / 75% PEG-b-DPB. These micelles will be referred to as 100D/no PEG, 75D/5k PEG, 50D/5k PEG, and 25D/5k PEG, respectively. For these four mixed micelles, the only difference in composition was the relative quantity of PEG and DMAEMA in the corona. Additionally, 50/50 micelles were made with the 10k and 20k PEG-containing PEG-b-DPB polymers mixed with the D-b-DPB to form 50D/10k PEG and 50D/20k PEG micelles.

Table 1. Molecular weight and composition of polymers used to create mixed micelles.

Polymer Name	Mn (g/mol)	PDI	Mn DMAEMA (g/mol)	Mn PEG (g/mol)	% BMA (core)	% DMAEMA (core)	% PAA (core)
D-b-DPB	32370	1.1	12200	N/A	52	21	27
5k PEG-b-DPB	26620	1.3	N/A	5000	45	25	30
10k PEG-b-DPB	31080	1.7	N/A	10000	45	26	29
20k PEG-b-DPB	55160	1.5	N/A	20000	47	28	25

Micelle characterization

The 100D/no PEG, 75D/5k PEG, 50D/5k PEG, and 25D/5k PEG micelles all had hydrodynamic diameters of ~35 nm (Figure 3A). However, micelle size increased for formulations with increased PEG molecular weight, ranging from 35 nm (50D/5k PEG) to 65 nm (50D/20k PEG) (Figure 3B). Generally, these diameters are in a useful range for EPR-based tumor delivery and are large enough to avoid renal clearance and small enough to avoid rapid macrophage clearance [29]. The ζ potential of the micelles is linearly correlated to the percent D-b-DPB in the 5 kDa PEG-containing mixed micelles, ranging from +17.6 mV (100D/no PEG) to +11.2 mV (75D/5k PEG) to +4.6 mV (50D/5k PEG) to +0.1 mV (25D/5k PEG). This trend suggests that the addition of PEG in the micelle corona causes surface charge shielding. Similarly, as the PEG molecular weight increases in the 50D micelles, the ζ potential decreases from +4.6 mV to +2.2 mV to +0.5 mV for the 5k, 10k, and 20k PEG-PDB polymers, respectively. These data suggest that both relative molar percent and molecular weight of the PEG molecule can effectively shield micelle surface charge.

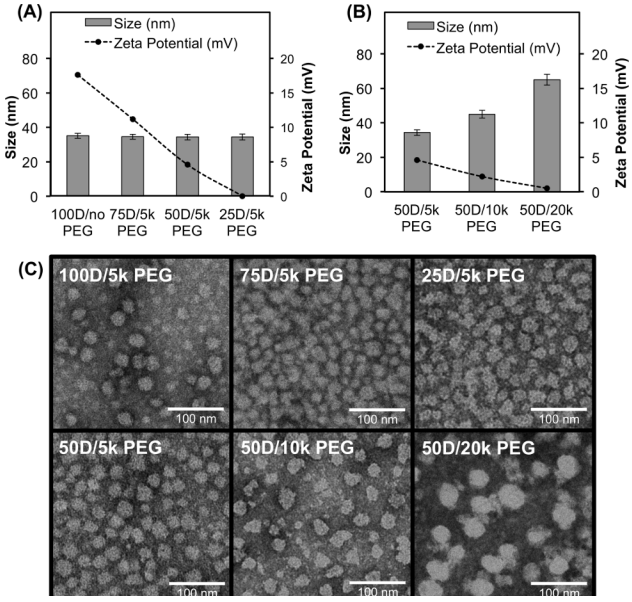

Figure 3. Chemicophysical characterization of mixed micelles. (A) Size and ζ potential of micelles containing variable mixtures PEG and pDMAEMA in the micelle corona, n = 3. (B) Size and ζ potential of 50D micelles containing varied lengths of PEG in the micelle corona, n = 3. (C) TEM of mixed micelles.

TEM images reflect the size of the dehydrated mixed micelles that contain a collapsed corona (Figure 3C) [28]. Micelle diameter remains constant for the micelles containing the 5k PEG coronas with a diameter of approximately 20 nm. Micelles with the 10 kDa and 20 kDa

PEG coronas have larger diameters of around 25 nm and 40 nm, respectively, which is consistent with the relative size increases measured with DLS (Figure 3C).

Micelle endosomal escape ability

Hemolysis was performed to confirm the mixed micelles' ability to escape the endosome upon cellular uptake (Figure 4). At pHs of 7.4 and 6.8, which represent cytoplasm and early endosome, the micelles show little to no hemolysis. As the pH decreases to that representative of the late endosome and lysosome (pH 6.2 and pH 5.6, respectively), percent hemolysis notably increases. This data indicates the potential for the mixed micelles to lyse the endosomal compartment before degradation in the late lysosome. This ability is crucial for intracellular delivery of siRNA.

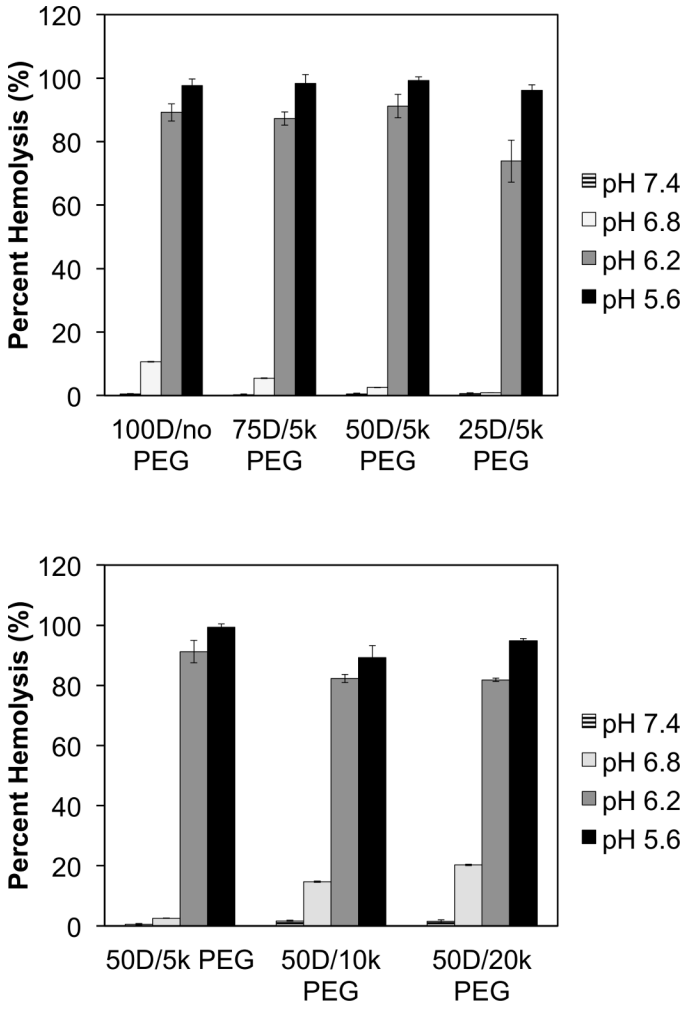

Figure 4. Hemolysis experiments determine endosomal escape abilities of mixed micelles. n = 3. (A) 5k PEG micelles with different molar compositions show hemolysis (B) 50D mixed micelles with different PEG lengths show hemolysis.

Micelle hemocompatibilty, stability, and siRNA protection

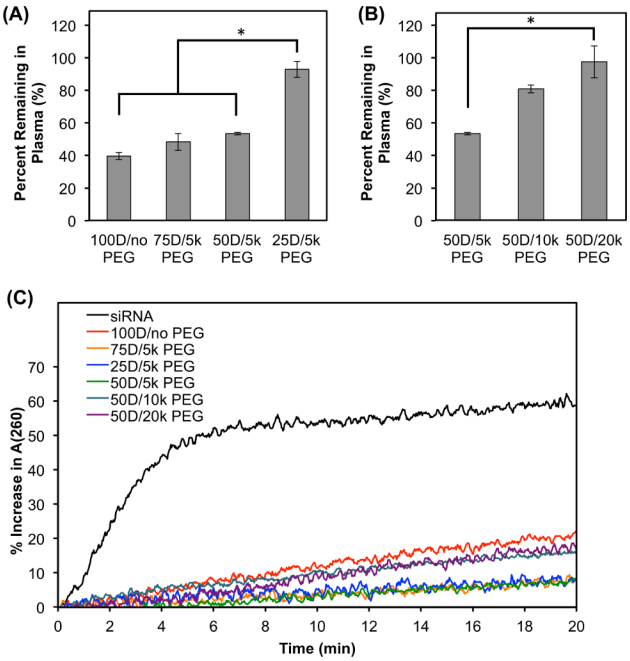

Figure 5. Characterization of mixed micelle hemocompatibilty, protection of siRNA against nucleases, and micelle stability in presence of heparin. (A) Hemocompatibilty of mixed micelles containing varied percentage molar composition of PEG on the micelle corona indicates an increase in percentage PEG results in more desirable hemocompatibilty. (B) Hemocompatibilty of 50D micelles containing varied lengths of PEG on the micelle corona show that longer PEG results in more desirable hemocompatibilty. (C) siRNA protection of mixed micelles against nucleases indicates the micelles effectively protect cargo against nucleases.

To predict *in vivo* translatability of these mixed micelles, their stability was measured upon exposure to human whole blood. Upon intravenous injection, cationic micelles are pre-disposed to adsorb blood serum proteins, which affects organ distribution and pharmacokinetics [30] and to form aggregates in the presence of serum proteins, which can cause an embolism within lung capillaries [12]. To model this phenomenon, Cy5-labeled dsDNA micelleplexes were incubated in fresh, anticoagulated whole human blood, and the percentage of micelles remaining in the plasma was quantified (Figure 5A and 5B) after incubation and a centrifugation step intended to separate out red blood cells and any micelle aggregates. Increasing the ratio of the PEG-b-DBP polymer relative to the D-b-DPB in the 5k PEG mixed micelles increased the percent of micelles remaining in the plasma supernatant; a significant portion (93%) of the 25D/5k PEG micelles remained in the plasma. PEG molecular weight also correlated with mixed micelle retention in the plasma supernatant, which ranged from 53% (50D/5k PEG) to 98% (50D/20k PEG). These trends are likely due to the charge shielding and decreased zeta potential achieved

by PEG addition. This *ex vivo* screening suggests that micelles with the longest or highest surface concentration of PEG would be the most hemocompatible for *in vivo* studies.

Another barrier to siRNA bioactivity *in vivo* is degradation and inactivation of siRNA by nucleases. The hyperchromic effect is the increase in absorbance at 260 nm (A(260)) upon nucleic acid degradation. siRNA protection by micelles was characterized by the hyperchromic effect during exposure to Riboshredder RNAse blend (Figure 5C). All of the mixed micelle formulations effectively protected the siRNA against degradation in comparison with siRNA alone. After 20 minutes, unformulated siRNA with the Riboshredder resulted in a 60% increase in A(260), while the siRNA formulated with the 100D/no PEG micelle exposed to Riboshredder resulted in the least protection among micelles, with an increase in A(260) of 20%. All of the mixed micelles effectively protect the siRNA from nuclease degradation *in vitro*, which is potentially predictive of similar benefit *in vivo*.

Cellular uptake and gene knockdown

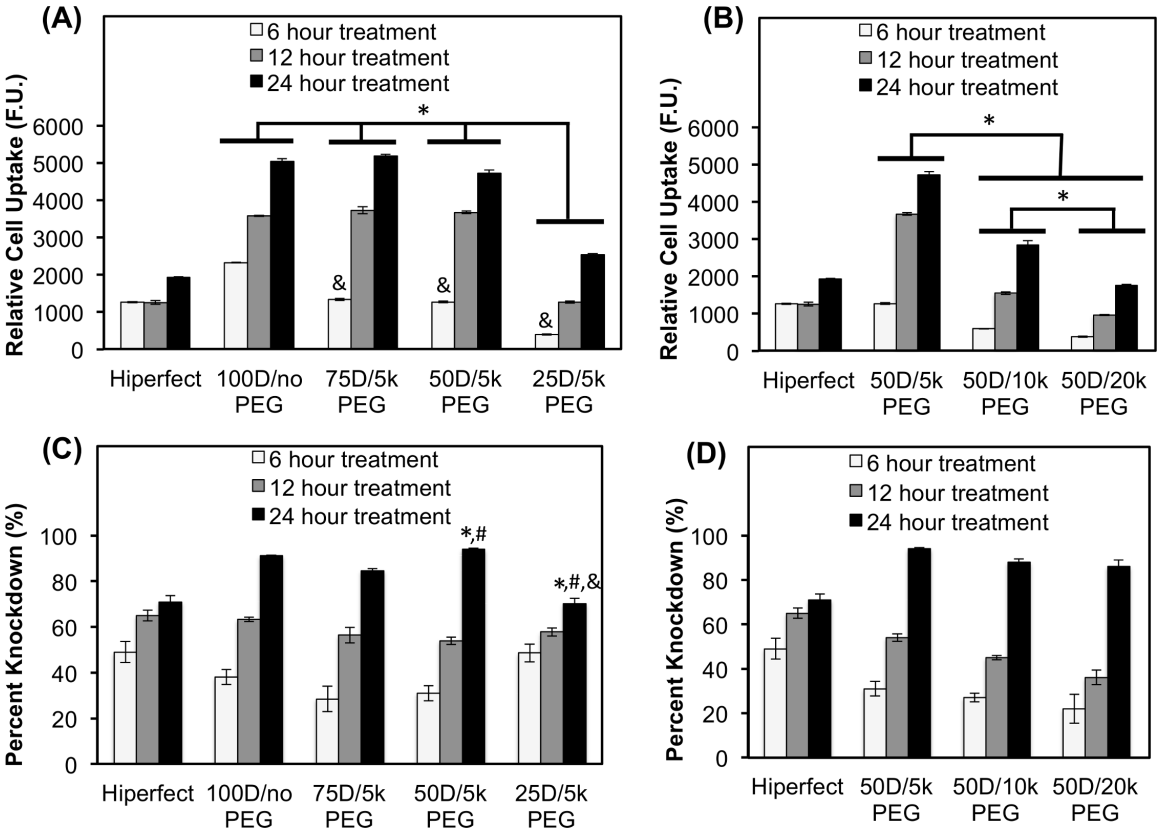

Figure 6. Cellular uptake and gene knockdown after different treatment times. (A) Relative cell uptake of mixed micelles containing varied ratios of PEG and DMAEMA in the corona. * $p < 0.05$ (I am not clear what comparisons are being *'d for A) and & indicates significant difference ($p < 0.05$) from 100D/no PEG. (B) Relative cell uptake of 50D micelles containing varied molecular weight of PEG in the corona. * $p < 0.05$. (C) Percent knockdown of model gene luciferase achieved by luciferase siRNA delivered via mixed micelles containing varied amounts of 5k PEG on the corona. * indicates significance ($p < 0.05$) from 100D/no PEG treatment; # indicates significance ($p < 0.05$) from 75D/5k PEG treatment; & indicates significance ($p < 0.05$) from 50D/5k PEG treatment. (D) Percent knockdown of model gene luciferase using siRNA delivered in 50D mixed micelles containing varied molecular weight of PEG in the corona.

Cellular uptake of Alexa488-labeled dsDNA mixed micelleplexes was evaluated by flow cytometry in MDA-MB-231 human mammary gland carcinoma cells (Figure 6A and Figure 6B). Regardless of mixed micelle stoichiometry, cellular uptake of dsDNA increased with treatment time. Cellular uptake tended to inversely correlate with the ratio of PEG/pDMAEMA and the molecular weight of PEG in the corona, which is especially apparent at the 6-hour treatment

time. Increasing the amount and molecular weight of the PEG also decreased zeta potential, which was likely a significant contributor to the differences in rate and extent of cellular uptake. This result is consistent with the presumption that electrostatic interactions between cationic delivery systems and the anionic cell surface promote internalization [7]. This relationship is especially apparent among different PEG lengths in the 50D formulations (Figure 6B). The 50D/5k PEG, 50D/10k PEG, and 50D/20k PEG micelles resulted in significantly different cellular uptake for each of the treatment times. Finely tuning the stoichiometry and PEG molecular weight of the mixed micelles can be utilized to optimize the micelleplexes with an ideal combination of hemo-stability and cellular uptake / gene silencing bioactivity.

RNAi was assessed in MDA-MB-231 cells that were lentivirally transduced to constitutively express luciferase. In contrast to cellular uptake, gene knockdown did not correlate as strongly to the amount of pDMAEMA in the micelleplex corona (Figure 6C and Figure 6D). PEG length in the 50D mixed micelles did not significantly influence gene knockdown, although cellular uptake was different among these micelles. A number of events required for efficient RNAi occur between cellular uptake and protein-level knockdown by siRNA, and a key step is unpackaging and release of the siRNA so that it can load into the RISC and mediate gene silencing.

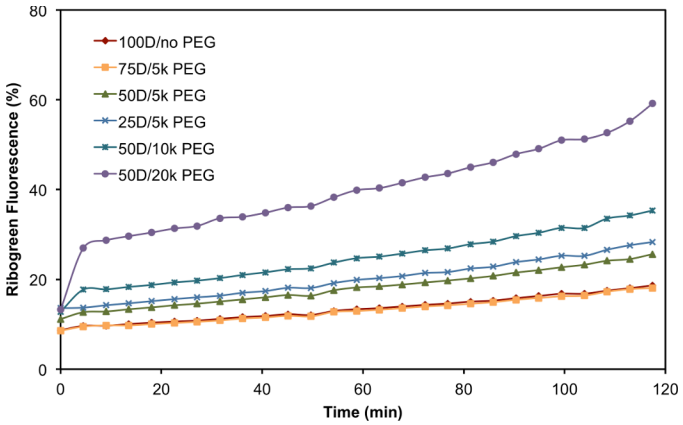

Figure 7. Kinetics of siRNA decomplexation from micelles after exposure to 250 U/L heparin at an siRNA concentration of 100 nM.

We hypothesized that larger percent PEG and larger molecular weight PEG may be better released intracellularly due to reduced charge density and reduced valency of the interactions between pDMAEMA and siRNA. This may enable efficient gene silencing with

these micelleplexes due to enhanced intracellular bioavailability, despite reduced rate of cell internalization [31].

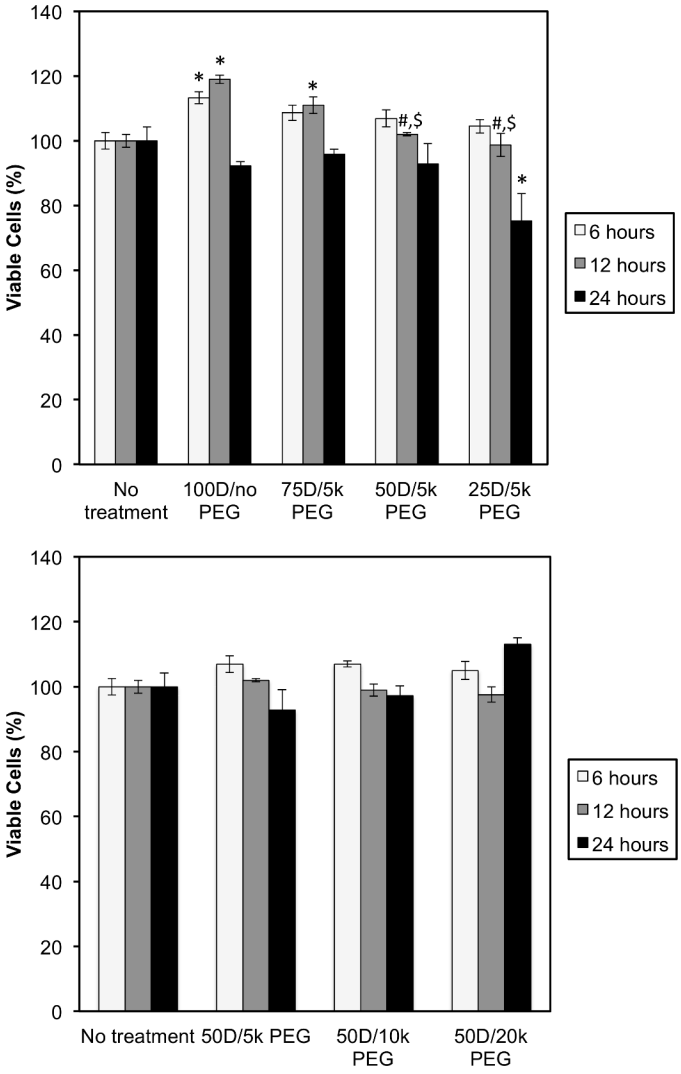

Figure 8. Cytotoxicity evaluation of mixed micelles at different treatment times at a siRNA dose of 100 nM. (A) Cell viability of NIH 3T3 cells after treatment with mixed micelles containing varied percent molar composition of PEG on the micelle corona. (B) Cell viability of NIH 3T3 cells after treatment with mixed micelles containing varied lengths of PEG on the micelle corona. * signifies significant difference from No Treatment ($p < 0.05$), # signifies significant difference from 100D/no PEG ($p < 0.05$), and $ signifies significant difference from 75D/5k PEG ($p < 0.05$)

In support of this hypothesis, micelles were exposed to the polyanion heparin, and siRNA unpackaging was measured using RiboGreen (Figure 7). Micelles with higher surface ratio and with larger molecular weight PEG on the corona resulted in a more rapid and complete siRNA release over two hours. This result is consistent with the hypothesis that the micelleplexes with the higher surface ratio and higher molecular weight PEG in the corona may release siRNA more efficiently intracellularly, resulting in a greater level of bioavailability / gene silencing relative to the quantity of siRNA internalized.

Cytotoxicity evaluation

A cytocompatibility study was performed in NIH 3T3 fibroblasts retrovirally transduced to constitutively express luciferase (Figure 8). The 25D/5k PEG micelleplex at the maximum treatment time of 24 hours showed a significant

25% cytotoxicity relative to untreated cells, while none of the other formulations at any treatment time caused a significant reduction in viable cell number. The mild toxicity of the 25D/5k PEG micelleplex can be attributed to the higher total amount of polymer required to make this formulation with siRNA at a charge ratio of 6:1. The charge ratio and siRNA concentration was held constant for all micelleplex formulations, but because the pD-b-PDB is the sole contributor to the charge ratio calculation, the total amount of polymer is increased as the % pDMAEMA is decreased in the micelleplex. While the 25D/5k PEG micelle is favorable for its low ζ potential, it requires a high polymer dose. This was motivation to expand the current study to also consider the larger molecular weight PEG molecules in order to achieve efficient charge shielding of the more cytocompatible 50D formulation.

In vivo blood circulation half-life and biodistribution

Because of the desirable properties observed for the 50D micelles, they were carried forward for

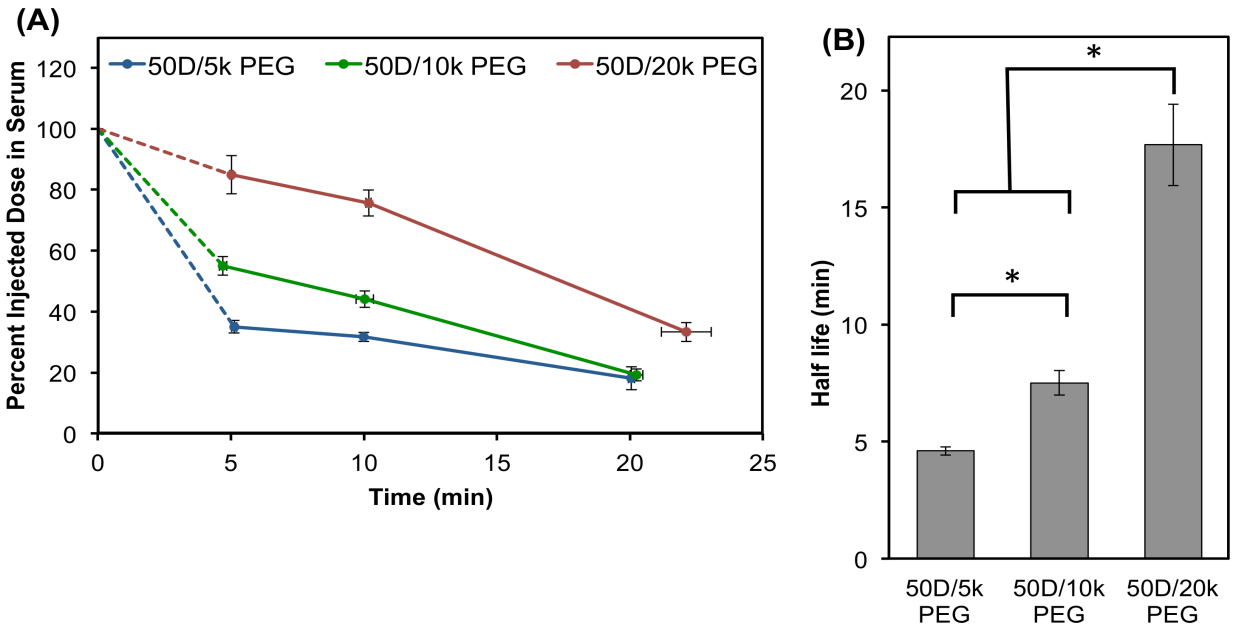

Figure 9. Effect of PEG length on corona on *in vivo* blood circulation half-life. (A) Concentration of 50D micelles with varied PEG lengths on the corona present in blood serum over time, n = 5. (B) Blood circulation half-life time values of 50D micelles with varied PEG lengths on corona. * represents significance ($p < 0.05$).

initial characterization *in vivo*. Extended blood circulation half-life is critical for effective tumor accumulation of nanomaterials by the EPR effect [32], [33]. Previous studies using cationic polymeric siRNA carriers achieve blood circulation half-life values of <5 minutes [14], [34]. Here, blood circulation half-life ($t_{1/2}$) was determined by collecting blood at known times, and fitting the data to a one-variable exponential model that assumes starting dose (t = 0) in serum is 100%, $N(t) = 100 * e^{-t*ln(2)/t_{1/2}}$. Fitting the data to this model gives significantly different blood circulation half-lives of 4.6 minutes for 50D/5k PEG, 7.5 minutes for 50D/10k PEG, and 17.7 minutes for 50D/20k PEG (Figure 9). These data demonstrate that there is a strong dependence of blood circulation half-life on 50D micelle PEG molecular weight. This also implies that *in vivo* half-life and function of structurally identical micelles can be modulated simply by altering PEG molecular weight in the corona. The improved blood circulation half-life of the 50D/20k PEG micelle may also result in improved tissue biodistribution following injection

Biodistribution of the micelleplexes was evaluated in the mice postmortem. Fluorescent imaging of organs (Figure 10B) confirmed that, as expected, a large percentage of the nanocarriers accumulated within the liver for all 50D mixed micelles. The 50D/5k PEG micelles had significantly greater biodistribution to the lungs, which is consistent with the *ex vivo* hemo-stability data

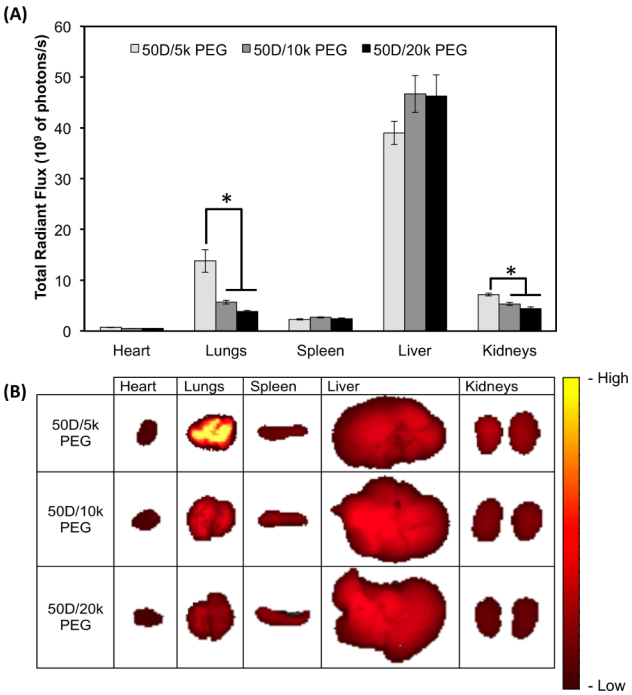

Figure 10. *In vivo* tissue distribution of 50D micelles containing varied PEG lengths on the micelle corona 20 minutes after injection in BALB/c mice. (A) Total fluorescence of the 50D micelles in 5 main organs, n = 8. * represents significance (p < 0.05). (B) Representative images of fluorescent biodistribution in 5 main organs.

in Figure 2. The 50D/5k PEG micelles resulted in a 2-fold increase in fluorescence in the lungs compared to the 50D/10k PEG micelles, and a 4-fold increase compared to the 50D/20k PEG micelles. Increasing the PEG molecular weight minimized micelle biodistribution in the lungs, which would be predicted to decrease any potential for longer-term carrier toxicity *in vivo*. Similarly, increasing PEG molecular weight also affected biodistribution in the kidneys, and the 50D/5k PEG micelleplexes had significantly increased distribution in the kidneys relative to the 50D/10k PEG and the 50D/20k PEG micelleplexes. This implies the 50D/5k PEG micelles may be more readily destabilized in the blood circulation, resulting in siRNA unpackaging and rapid renal clearance of the free molecules. Tissue distribution was generally as expected for the 50D/20k PEG micelleplexes, and their extended circulation time suggests that they may be ideal for tumor targeting in vivo.

CHAPTER IV

CONCLUSIONS

In vitro analysis was performed on a series of mixed micelles that contain varying surface concentrations and molecular weights of PEG on the corona to shield the micelles' cationic charge. The micelles that contained the highest surface concentration and the largest molecular weight PEG showed the least adsorption to blood plasma proteins *ex vivo.* These particles also showed the lowest cellular uptake in MDA-MB-231 mammary gland carcinoma cells, likely due to the charge shielding that is achieved with the addition of PEG. The series of mixed micelles demonstrated similar levels of gene silencing *in vitro,* implying different micelles undergo different intracellular processing following cellular uptake, likely due to their surface charge density.

Ultimately, micelles with varying molecular weight PEG on the corona were chosen for further *in vivo* analysis based on their compatibility characteristics and their efficacy *in vitro*. Increased PEG molecular weight corresponded to decreased micelle accumulation in the kidneys and the lungs, which suggests a significant improvement in stability and decreased blood cell aggregation that leads to embolism, respectively. Increased PEG length corresponded to a significantly longer blood circulation half-life. Longer half-life is desirable because it allows the micelles to reach the intended tissue more readily without being prematurely cleared.

The 50D/20k PEG micelle demonstrates the potential for biocompatible siRNA delivery. The long blood circulation half-life can be leveraged for delivery of therapeutic siRNA to tumors that are vascularized with the EPR effect. Ongoing studies will assess the 50D/20k formulation for siRNA delivery to orthotropic breast cancer tumors that possess EPR

characteristics. It is expected that due to the micelle's desirable properties, as evaluated *in vitro* and *in vivo*, it will preferentially distribute to the tumor and will effectively mediate RNAi in the tumor. The present study has introduced a neutralized micelle that shows promise as a safe, stable *in vivo* siRNA delivery platform that will be evaluated further.

REFERENCES

[1] G. Meister and T. Tuschl, “Mechanisms of gene silencing by double-stranded RNA.,” *Nature*, vol. 431, no. 7006, pp. 343–9, Sep. 2004.

[2] C. P. Paul, P. D. Good, I. Winer, and D. R. Engelke, “Effective expression of small interfering RNA in human cells.,” *Nat. Biotechnol.*, vol. 20, no. 5, pp. 505–8, May 2002.

[3] K. A. Whitehead, R. Langer, and D. G. Anderson, “Knocking down barriers: advances in siRNA delivery.,” *Nat. Rev. Drug Discov.*, vol. 8, no. 2, pp. 129–38, Feb. 2009.

[4] R. Kanasty, J. R. Dorkin, A. Vegas, and D. Anderson, “Delivery materials for siRNA therapeutics.,” *Nat. Mater.*, vol. 12, no. 11, pp. 967–77, Oct. 2013.

[5] “Reich, Mol Vis 2003; 9:210-216.” [Online]. Available: http://www.molvis.org/molvis/v9/a31/.

[6] R. L. Kanasty, K. A. Whitehead, A. J. Vegas, and D. G. Anderson, “Action and reaction: the biological response to siRNA and its delivery vehicles.,” *Mol. Ther.*, vol. 20, no. 3, pp. 513–24, Mar. 2012.

[7] B. Urban-Klein, S. Werth, S. Abuharbeid, F. Czubayko, and A. Aigner, “RNAi-mediated gene-targeting through systemic application of polyethylenimine (PEI)-complexed siRNA in vivo.,” *Gene Ther.*, vol. 12, no. 5, pp. 461–6, Mar. 2005.

[8] L. Wightman, R. Kircheis, V. Rössler, S. Carotta, R. Ruzicka, M. Kursa, and E. Wagner, “Different behavior of branched and linear polyethylenimine for gene delivery in vitro and in vivo.,” *J. Gene Med.*, vol. 3, no. 4, pp. 362–72.

[9] R. Shrestha, M. Elsabahy, S. Florez-Malaver, S. Samarajeewa, and K. L. Wooley, “Endosomal escape and siRNA delivery with cationic shell crosslinked knedel-like nanoparticles with tunable buffering capacities,” *Biomaterials*, vol. 33, no. 33, pp. 8557–8568, 2012.

[10] D. Reischl and A. Zimmer, “Drug delivery of siRNA therapeutics: potentials and limits of nanosystems,” *Nanomedicine Nanotechnology, Biol. Med.*, vol. 5, no. 1, pp. 8–20, 2009.

[11] S. Dokka, D. Toledo, X. Shi, V. Castranova, and Y. Rojanasakul, “Oxygen Radical-Mediated Pulmonary Toxicity Induced by Some Cationic Liposomes,” *Pharm. Res.*, vol. 17, no. 5, pp. 521–525, May 2000.

[12] S. A. L. Audouy, L. F. M. H. de Leij, D. Hoekstra, and G. Molema, “In Vivo Characteristics of Cationic Liposomes as Delivery Vectors for Gene Therapy,” *Pharm. Res.*, vol. 19, no. 11, pp. 1599–1605, Nov. 2002.

[13] B. M. Brenner, T. H. Hostetter, and H. D. Humes, "Glomerular permselectivity: barrier function based on discrimination of molecular size and charge," *Am J Physiol Ren. Physiol*, vol. 234, no. 6, pp. F455–460, Jun. 1978.

[14] J. E. Zuckerman, C. H. J. Choi, H. Han, and M. E. Davis, "Polycation-siRNA nanoparticles can disassemble at the kidney glomerular basement membrane.," *Proc. Natl. Acad. Sci. U. S. A.*, vol. 109, no. 8, pp. 3137–42, Feb. 2012.

[15] A. J. Convertine, D. S. W. Benoit, C. L. Duvall, A. S. Hoffman, and P. S. Stayton, "Development of a novel endosomolytic diblock copolymer for siRNA delivery," *J. Control. Release*, vol. 133, no. 3, pp. 221–229, 2009.

[16] A. J. Convertine, C. Diab, M. Prieve, A. Paschal, A. S. Hoffman, P. H. Johnson, and P. S. Stayton, "pH-Responsive Polymeric Micelle Carriers for siRNA Drugs.," *Biomacromolecules*, vol. 11, no. 11, pp. 2904–2911, Oct. 2010.

[17] R. S. Burke and S. H. Pun, "Extracellular barriers to in Vivo PEI and PEGylated PEI polyplex-mediated gene delivery to the liver.," *Bioconjug. Chem.*, vol. 19, no. 3, pp. 693–704, Mar. 2008.

[18] T. Maldiney, C. Richard, J. Seguin, N. Wattier, M. Bessodes, and D. Scherman, "Effect of core diameter, surface coating, and PEG chain length on the biodistribution of persistent luminescence nanoparticles in mice.," *ACS Nano*, vol. 5, no. 2, pp. 854–62, Feb. 2011.

[19] V. C. F. Mosqueira, P. Legrand, J.-L. Morgat, M. Vert, E. Mysiakine, R. Gref, J.-P. Devissaguet, and G. Barratt, "Biodistribution of Long-Circulating PEG-Grafted Nanocapsules in Mice: Effects of PEG Chain Length and Density," *Pharm. Res.*, vol. 18, no. 10, pp. 1411–1419, Oct. 2001.

[20] S. Khargharia, K. Kizzire, M. D. Ericson, N. J. Baumhover, and K. G. Rice, "PEG length and chemical linkage controls polyacridine peptide DNA polyplex pharmacokinetics, biodistribution, metabolic stability and in vivo gene expression," *J. Control. Release*, vol. 170, no. 3, pp. 325–333, 2013.

[21] P. R. Dash, M. L. Read, L. B. Barrett, M. A. Wolfert, and L. W. Seymour, "Factors affecting blood clearance and in vivo distribution of polyelectrolyte complexes for gene delivery.," *Gene Ther.*, vol. 6, no. 4, pp. 643–50, Apr. 1999.

[22] H. Maeda, Y. Matsumura, J. Fang, H. Nakamura, and H. Maeda, "The EPR effect: Unique features of tumor blood vessels for drug delivery, factors involved, and limitations and augmentation of the effect," *Adv. Drug Deliv. Rev.*, vol. 63, no. 3, pp. 136–151, 2011.

[23] C. E. Nelson, M. K. Gupta, E. J. Adolph, J. M. Shannon, S. A. Guelcher, and C. L. Duvall, "Sustained local delivery of siRNA from an injectable scaffold.," *Biomaterials*, vol. 33, no. 4, pp. 1154–61, Feb. 2012.

[24] B. C. Evans, C. E. Nelson, S. S. Yu, K. R. Beavers, A. J. Kim, H. Li, H. M. Nelson, T. D. Giorgio, and C. L. Duvall, "Ex vivo red blood cell hemolysis assay for the evaluation of pH-responsive endosomolytic agents for cytosolic delivery of biomacromolecular drugs.," *J. Vis. Exp.*, no. 73, p. e50166, Jan. 2013.

[25] C. E. Nelson, J. R. Kintzing, A. Hanna, J. M. Shannon, M. K. Gupta, and C. L. Duvall, "Balancing Cationic and Hydrophobic Content of PEGylated siRNA Polyplexes Enhances Endosome Escape, Stability, Blood Circulation Time, and Bioactivity in Vivo.," *ACS Nano*, vol. 7, no. 10, pp. 8870–80, Oct. 2013.

[26] S. Kirkland-York, Y. Zhang, A. E. Smith, A. W. York, F. Huang, and C. L. McCormick, "Tailored design of Au nanoparticle-siRNA carriers utilizing reversible addition-fragmentation chain transfer polymers.," *Biomacromolecules*, vol. 11, no. 4, pp. 1052–9, Apr. 2010.

[27] S. S. Yu, C. M. Lau, W. J. Barham, H. M. Onishko, C. E. Nelson, H. Li, C. A. Smith, F. E. Yull, C. L. Duvall, and T. D. Giorgio, "Macrophage-specific RNA interference targeting via 'click', mannosylated polymeric micelles.," *Mol. Pharm.*, vol. 10, no. 3, pp. 975–87, Mar. 2013.

[28] H. Li, S. S. Yu, M. Miteva, C. E. Nelson, T. Werfel, T. D. Giorgio, and C. L. Duvall, "Matrix Metalloproteinase Responsive, Proximity-Activated Polymeric Nanoparticles for siRNA Delivery," *Adv. Funct. Mater.*, vol. 23, no. 24, pp. 3040–3052, Jun. 2013.

[29] F. Alexis, E. Pridgen, L. K. Molnar, and O. C. Farokhzad, "Factors affecting the clearance and biodistribution of polymeric nanoparticles.," *Mol. Pharm.*, vol. 5, no. 4, pp. 505–15, Jan. 2008.

[30] D. Y. Furgeson, M. A. Dobrovolskaia, P. Aggarwal, J. B. Hall, C. B. McLeland, M. A. Dobrovolskaia, and S. E. McNeil, "Nanoparticle interaction with plasma proteins as it relates to particle biodistribution, biocompatibility and therapeutic efficacy," *Adv. Drug Deliv. Rev.*, vol. 61, no. 6, pp. 428–437, 2009.

[31] S. Mao, M. Neu, O. Germershaus, O. Merkel, J. Sitterberg, U. Bakowsky, and T. Kissel, "Influence of polyethylene glycol chain length on the physicochemical and biological properties of poly(ethylene imine)-graft-poly(ethylene glycol) block copolymer/SiRNA polyplexes.," *Bioconjug. Chem.*, vol. 17, no. 5, pp. 1209–18, Jan. 2006.

[32] H. Maeda, Y. Matsumura, and V. Torchilin, "Tumor delivery of macromolecular drugs based on the EPR effect," *Adv. Drug Deliv. Rev.*, vol. 63, no. 3, pp. 131–135, 2011.

[33] G. Kwon, S. Suwa, M. Yokoyama, T. Okano, Y. Sakurai, and K. Kataoka, "Enhanced tumor accumulation and prolonged circulation times of micelle-forming poly (ethylene oxide-aspartate) block copolymer-adriamycin conjugates," *J. Control. Release*, vol. 29, no. 1, pp. 17–23, 1994.

[34] B. Naeye, H. Deschout, V. Caveliers, B. Descamps, K. Braeckmans, C. Vanhove, J. Demeester, T. Lahoutte, S. C. De Smedt, and K. Raemdonck, “In vivo disassembly of IV administered siRNA matrix nanoparticles at the renal filtration barrier,” *Biomaterials*, vol. 34, no. 9, pp. 2350–2358, 2013.